Original Article

Enhancing the accuracy of genioplasty using mixed reality and computer-aided design/manufacturing: a randomized controlled trial

Kotaro Tachizawa[1]^, Keisuke Sugahara[1,2], Masahide Koyachi[1], Kento Odaka[2,3], Satoru Matsunaga[2,4], Maki Sugimoto[1,5], Akira Katakura[1,2]

[1]Department of Oral Pathobiological Science and Surgery, Tokyo Dental College, Tokyo, Japan; [2]Oral Health Science Center, Tokyo Dental College, Tokyo, Japan; [3]Department of Oral and Maxillofacial Radiology, Tokyo Dental College, Tokyo, Japan; [4]Department of Anatomy, Tokyo Dental College, Tokyo, Japan; [5]Innovation Lab, Teikyo University Okinaga Research Institute, Tokyo, Japan

Contributions: (I) Conception and design: K Tachizawa, K Sugahara, M Koyachi, K Odaka, S Matsunaga, A Katakura; (II) Administrative support: K Tachizawa, K Sugahara, M Koyachi, M Sugimoto; (III) Provision of study materials or patients: K Sugahara, M Koyachi, K Odaka; (IV) Collection and assembly of data: K Tachizawa, K Sugahara, M Koyachi, S Matsunaga; (V) Data analysis and interpretation: K Tachizawa, K Sugahara, M Koyachi; (VI) Manuscript writing: All authors; (VII) Final approval of manuscript: All authors.

Correspondence to: Akira Katakura, DDS, PhD. Department of Oral Pathobiological Science and Surgery, Tokyo Dental College, 2-9-18 Kanda Misaki-cho, Chiyoda-ku, Tokyo 101-0061, Japan; Oral Health Science Center, Tokyo Dental College, Tokyo, Japan. Email: katakura@tdc.ac.jp.

Background: Genioplasty is performed as part of orthognathic surgery to correct jaw deformities. This procedure presents challenges in terms of osteosynthesis accuracy. This study aimed to evaluate the precision of preoperative planning in genioplasty using computer-aided design/computer-aided manufacturing (CAD/CAM) with three-dimensional (3D) printable biomaterials and mixed reality (MR) technology with a head-mounted display (Microsoft® HoloLens 2) and a registration marker.

Methods: Twenty-six patients underwent genioplasty using either only CAD/CAM devices (control group, n=10) or CAD/CAM with additional MR technology (experimental group, n=16). CAD/CAM devices were created based on virtual surgical planning (VSP), and MR holograms created based on VSP data were projected onto the surgical area using Microsoft HoloLens 2. After surgery, the planned model was compared with the postoperative computed tomography (CT) image, measuring the 3D surface and the differences in position and rotation using the root mean square deviation (RMSD) and Bland-Altman's method. Both analyses are blinded.

Results: The average 3D surface analysis errors within 2 mm ranged between 62.20–100.00% (control group) and 99.30–100.00% (experimental group), with mean errors of 92.12% and 99.81%, respectively. Errors within 1 mm ranged between 28.50–98.90% (control group) and 55.10–99.6% (experimental group) with mean errors of 67.36% and 85.60%, respectively. The largest RMSDs were 1.20 mm in the anteroposterior direction and 6.78° in pitch orientation for the experimental group and 1.78 mm in the anteroposterior direction and 6.04° in pitch orientation for the control group. A statistically significant difference between the two groups was observed for errors measured within 1 mm (P=0.047) and for yaw (P=0.003). No postoperative complications were observed in either group.

Conclusions: Using CAD/CAM with additional MR technology in genioplasty improved the repositioning accuracy of the chin bone fragment and plate placement, with statistically significant improvements in specific spatial directions. This combination of CAD/CAM and MR technology allows for intraoperative spatial verification of fragment movement according to preoperative VSP, which significantly contributes surgical precision.

^ ORCID: 0009-0000-1537-5620.

Keywords: Computer-aided design/computer-aided manufacturing (CAD/CAM); mixed reality (MR); genioplasty; three-dimensional analysis (3D analysis); three-dimensional printing (3D printing)

Submitted Oct 26, 2024. Accepted for publication Mar 12, 2025. Published online Apr 10, 2025.
doi: 10.21037/qims-24-2333
View this article at: https://dx.doi.org/10.21037/qims-24-2333

Introduction

Genioplasty is an orthognathic surgery widely used alone or in combination with osteotomies of the jaw to correct deformities of the chin (1). The osteotomy line and repositioning position are the most important factors in genioplasty, particularly in sliding genioplasty. The surgical procedure involves separating the chin fragment bone from the mandible and moving it to an ideal three-dimensional (3D) position for fixation. Operating while evaluating intraoperative soft tissue is challenging because the patient is under muscle relaxation and in a supine position during surgery. The ideal soft tissue was reproduced by recreating the position of hard tissue that moved during the preoperative simulation. Therefore, the position of hard tissue, such as the chin bone fragment, is essential for genioplasty. Additionally, genioplasty carries risks of complications, including mental nerve damage and postoperative sensory disturbance, as osteotomy is performed near the mental foramen (2-4). Conventional genioplasty relies heavily on the surgeon's experience, skills, sensibility, and intraoperative evaluation to determine the osteotomy line, amount of chin fragment movement, and plate fixation (5,6). Therefore, preoperative planning is not reproducible, and intraoperative 3D confirmation is extremely difficult (6,7). In addition, the evidence for cosmetic improvement or functional evaluation is limited. In recent years, digital transformation has accelerated in oral and maxillofacial surgery, and the use of digital technology and equipment has rapidly spread in this field (8-13). 3D printers are widely used in multiple fields, particularly orthognathic surgery. These printers use 3D printable biomaterials to create surgical devices using computer-aided design/computer-aided manufacturing (CAD/CAM) technology to improve the accuracy and safety of surgery and reduce the surgical time (7,14). A study has described the use of 3D devices to support genioplasty (7). The mainstream methods combine osteotomy and repositioning devices that accurately reproduce 3D movements. However, confirming the preoperatively planned movement of the chin fragment is difficult. Mixed reality (MR) technology equipped with a head-mounted display (HMD), such as Microsoft® HoloLens 2, is evolving and has been shown to improve the safety and accuracy of surgery as an alternative to a surgical navigation system. Chiacchiaretta reported that the use of MR technology for brain tumor surgery improved the accuracy and safety of the procedure (15). We previously reported the usefulness of MR in various oral surgeries (8,16-18). To date, no studies have verified the accuracy of genioplasty using CAD/CAM or MR (19,20).

In this study, we validated a novel genioplasty approach using CAD/CAM technology and MR surgical navigation with a novel HMD registration marker to improve the reproducibility and accuracy of virtual surgical planning (VSP) for repositioning the chin bone fragment during genioplasty (21). We present this article in accordance with the CONSORT reporting checklist (available at https://qims.amegroups.com/article/view/10.21037/qims-24-2333/rc).

Methods

The procedure in this study was conducted using six steps, which are outlined below and shown in *Figure 1*: (I) acquisition of the skull data from the computed tomography (CT) and teeth dentition data from intraoral optical scanning; (II) treatment planning via the creation of a skull-dental composite 3D model and a digital dental model and VSP; (III) fabrication of 3D devices and creation of the Microsoft® HoloLens 2 application; (IV) performance of the actual operation based on the VSP; and (V) evaluation of the accuracy of the operation by comparing the VSP with the postoperative CT outcomes. This study was conducted in accordance with the Declaration of Helsinki (as revised in 2013). This study was approved by the Ethics Committee of Tokyo Dental College (No. 794, 844) and informed consent was obtained from all individual participants. Since this study does not fall under the category of clinical trials requiring registration, it was not registered on a trial registry platform.

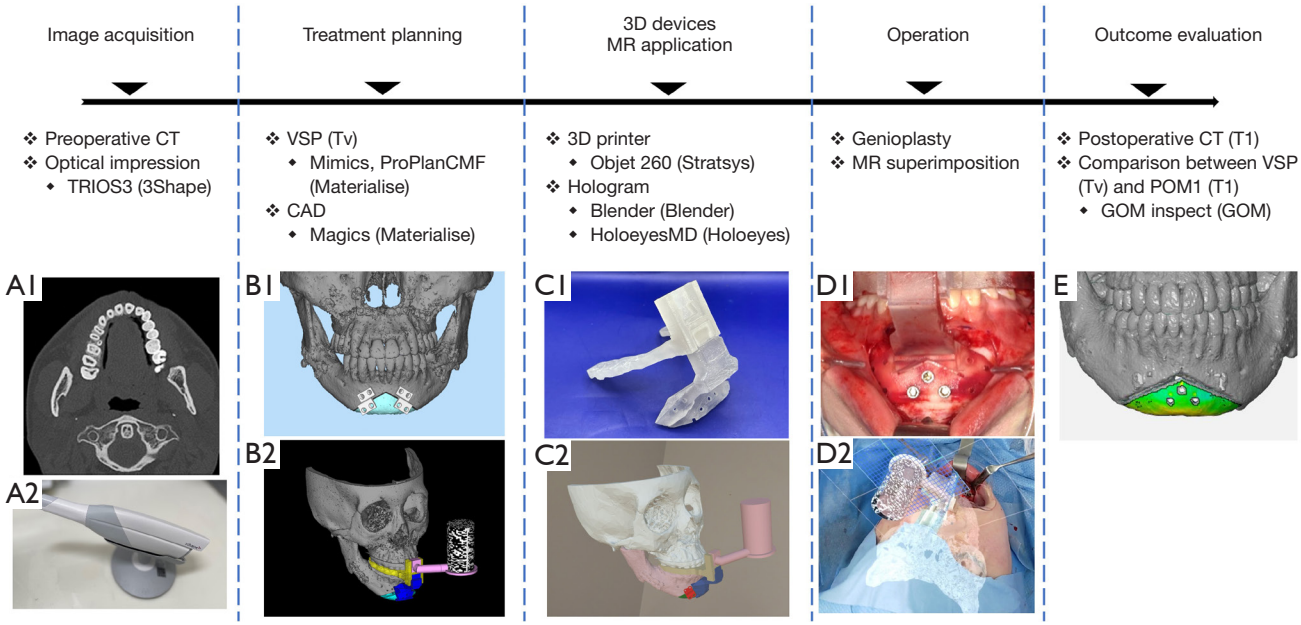

Figure 1 The workflow of this study: (A1) preoperative CT and (A2) TRIOS3 (3Shape) for optical impression; (B1) Mimics, ProplanCMF (Materialise) for VSP and (B2) Magics (Materialise) for CAD; (C1) 3D printer product by Objet 260 (Stratsys) and (C2) MR application by Holoeyes MD (Holoeyes); (D1) intraoperative view in genioplasty and (D2) MR superimposition; and (E) postoperative comparison between VSP and postoperative CT in 1 month by GOM Inspect (GOM). CAD, computer-aided design; CT, computed tomography; MR, mixed reality; POM1, postoperative month 1; T1, postoperative outcome; 3D, three-dimensional; Tv, the actual postoperative outcome; VSP, virtual surgical planning.

Study population

The details of the study population are given in *Table 1*. Twenty-six patients (3 men and 23 women) who underwent genioplasty alone at the Oral Surgery Department of Suidobashi Hospital, Tokyo Dental College, between April 2019 and August 2023, and consented to participate in this study. Their ages ranged between 20–56 years, with a mean age of 32.0 years. Patients who underwent genioplasty simultaneously with another orthognathic surgery or cleft palate and craniofacial anomaly correction were also excluded. Patients were classified into two groups: control (only CAD/CAM technology, n=10) and experimental (additional MR technology, n=16). This study was designed as a single-center randomized controlled clinical trial. Randomization was conducted using computer-generated allocation, ensuring equal assignment probability (*Figure 2*). Allocation concealment was maintained using sealed, opaque, sequentially numbered envelopes prepared by an independent third party. The envelopes were opened only after participant enrollment and baseline data collection, preserving sequence concealment until intervention assignment.

Image acquisition

CT scans (SOMATOM Definition AS; Siemens Healthineers, Forchheim, Germany) were obtained one month before surgery, and the CT images were formatted as Digital Imaging and Communications in Medicine (DICOM) data. Accurate reconstruction of the dentition is difficult owing to orthodontic brackets and prosthetic artifacts; therefore, optical impressions (Trios; 3Shape, Copenhagen, Denmark) of the occlusal surface morphology were obtained and converted into Standard Tessellation Language (STL) files. The data were transferred to Mimics (Materialize, Leuven, Belgium) and set up for VSP.

Preoperative procedure—VSP and 3D devices

The following software were used to create the 3D devices: Mimics (Materialize, Leuven, Belgium) for segmentation, ProPlanCMF (Materialize, Leuven, Belgium) for VSP, and Magics (Materialize, Leuven, Belgium) for CAD. The CT data were aligned with the tooth profile using ProPlanCMF, and the 3D-CT images were reconstructed

Table 1 Clinical information of the study patients and results of the 3D surface analysis

Patient	Age (years)	Diagnosis	Surgical treatment for chin	Error <2 mm	Error <1 mm
Control group (CAD/CAM)					
1	26	Asymmetry, retrogenia	Advancement, upward, rotation	62.15%	28.45%
2	32	Retrogenia	Advancement, upward	98.70%†	92.85%†
3	26	Retrogenia	Advancement, upward	100.00%†	85.85%
4	34	Retrogenia	Advancement	99.15%†	58.10%
5	20	Asymmetry, retrogenia	Advancement, rotation	100.00%†	76.00%
6	30	Retrogenia	Advancement	96.00%†	51.15%
7	43	Retrogenia	Advancement, upward	67.00%	39.20%
8	36	Antegenia	Setback, upward	100.00%†	84.95%
9	27	Antegenia	Upward	99.95%†	98.90%†
10	34	Antegenia	Setback, upward	98.20%†	58.10%
Experimental group (CAD/CAM + MR)					
11	27	Asymmetry, retrogenia	Advancement, upward	100.00%†	91.70%†
12	41	Retrogenia	Advancement	100.00%†	86.60%
13	24	Asymmetry, antegenia	Setback, right shift, upward, rotation	99.85%†	66.60%
14	28	Antegenia	Setback	99.85%†	92.15%†
15	20	Asymmetry	Right shift, rotation	99.25%†	90.65%†
16	56	Asymmetry, retrogenia	Advancement, upward, right shift	99.95%†	74.80%
17	32	Antegenia	Upward	100.00%†	96.45%†
18	28	Asymmetry, antegenia	Setback, rotation	99.55%†	90.85%†
19	21	Retrogenia	Advancement, upward	99.90%†	86.95%
20	48	Asymmetry, retrogenia	Advancement, upward, left shift	100.00%†	99.60%†
21	26	Antegenia	Upward	99.95%†	99.30%†
22	42	Antegenia	Upward	99.75%†	78.15%
23	49	Asymmetry, antegenia	Setback, left shift, rotation	99.30%†	55.10%
24	30	Asymmetry, antegenia	Setback, right shift, rotation	99.80%†	86.90%
25	23	Asymmetry, retrogenia	Advancement, left shift	99.80%†	83.30%
26	29	Antegenia	Advancement, upward	99.95%†	90.50%†

†, over 90%. 3D, three-dimensional; CAD/CAM, computer-aided design/computer-aided manufacturing; MR, mixed reality.

using the reverse data from the 0.6 mm slice-thick CT. The datasets were imported into the software, and automated Hounsfield unit (HU)-based segmentation was performed. The tooth-shape data were merged with the mandibular data using a wizard in ProPlanCMF. The osteotomy line was determined in consultation with the surgeon. The osteotomy devices, repositioning devices, splints, and positions of the registration markers were designed after discussing the amount of movement with the orthodontist and patient. The fixed plate was scanned and converted to STL format beforehand. Each 3D device was fabricated using a 3D printer (Objet 260 Connex; Stratasys Ltd., Eden Prairie, MN, USA) and a 3D printable biocompatible resin. The osteotomy and repositioning devices were fabricated to attach to the splint and be easily switched in and out at the junction site. No screws or adhesives were used at the joint

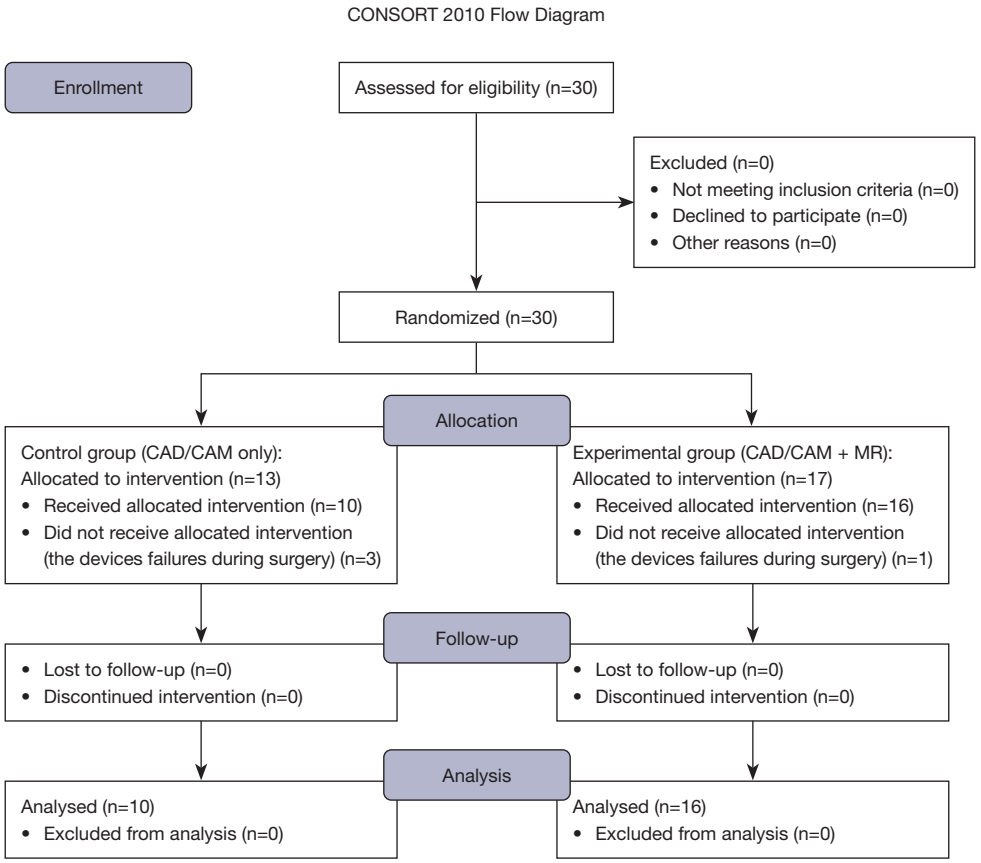

Figure 2 This flowchart illustrates participant enrollment, group allocation, and follow-up. Patients were randomized into the control group (CAD/CAM only, n=10) or the experimental group (CAD/CAM + MR, n=16). Postoperative accuracy was assessed using 3D surface and point-based analyses. 3D, three-dimensional; CAD/CAM, computer-aided design/computer-aided manufacturing; MR, mixed reality.

site; instead, a 'Koshikake aritsugi' (i.e., a stepped dovetail splice) configuration, which is used in shrine carpentry techniques, was applied (22).

Figure 3 shows the devices used in this study. Four types of devices were designed based on the VSP: a surgical splint with connectors, an osteotomy device (*Figure 3A*), a repositioning device (*Figure 3B*), and a registration marker (*Figure 3C*). These devices were fabricated using a PolyJet 3D printer (Objet 260 Connex, Stratasys, Eden Prairie, USA) with biocompatible resin (MED 610, Stratasys, Eden Prairie, USA) (*Figure 4*). The splint was designed by removing a simple shape from the region, including the interproximal space below the orthodontic brackets of the anterior teeth. A dovetail joint was used to connect the splint, the osteotomy device, repositioning device, and registration marker. The upper part of the osteotomy and repositioning devices contained space to avoid interference from the inverted flap.

The osteotomy device contains a slit in the ultrasonic cutting instrument that reflects the osteotomy line. Three drilling guide holes were placed in the center, contacting the mandibular surface for repositioning screws with a diameter of 2 mm, the same as the fixing temporary screws. Two drilling guide holes were designed to reposition the screws on both sides of the osteotomy line. The holes were positioned to reflect the plating position assumed during the preoperative simulation. A surface that matched the shape of the mandible after movement and three holes with a 2 mm diameter for repositioning the screws were designed in the center of the repositioning device (*Figure 4*).

Surgical procedures

All surgeries were performed by the same three oral and maxillofacial specialists in both groups. The surgery was performed by three surgeons who had been qualified as

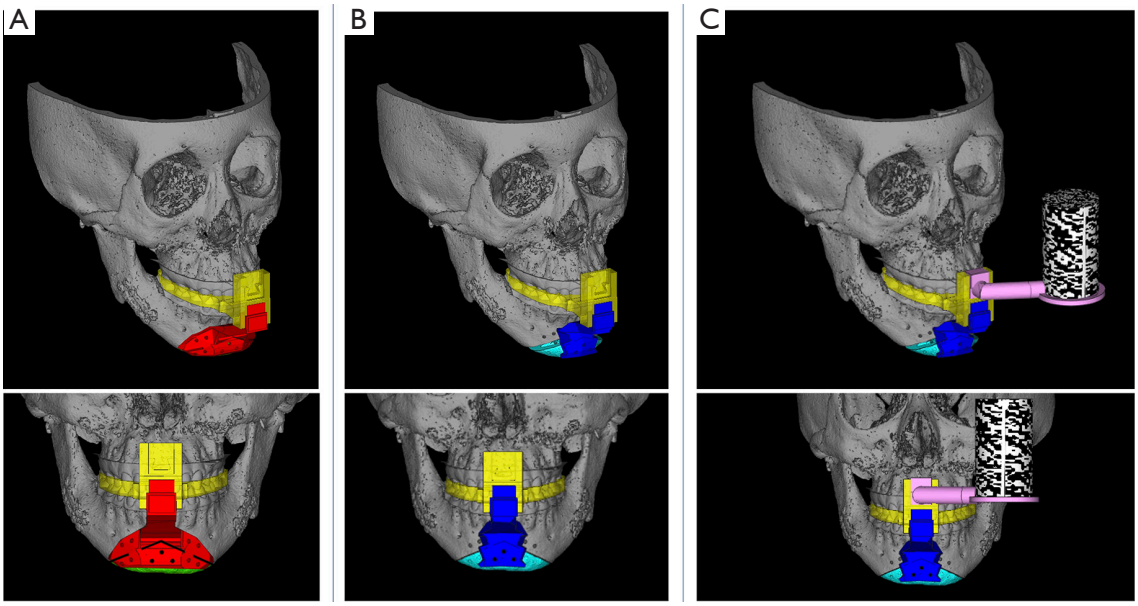

Figure 3 Computer-aided design of the three-dimensional devices: (A) splint (yellow) and osteotomy device (red); (B) repositioning device (blue); (C) registration marker (pink and monochrome mosaic); the osteotomy and repositioning devices were made to be attached to the splint and switched in or out at the lower junction site. The registration marker could be attached to the upper junction site. The highlighted areas represent the chin bone fragment. They are color-coded to indicate its condition immediately after osteotomy and after repositioning.

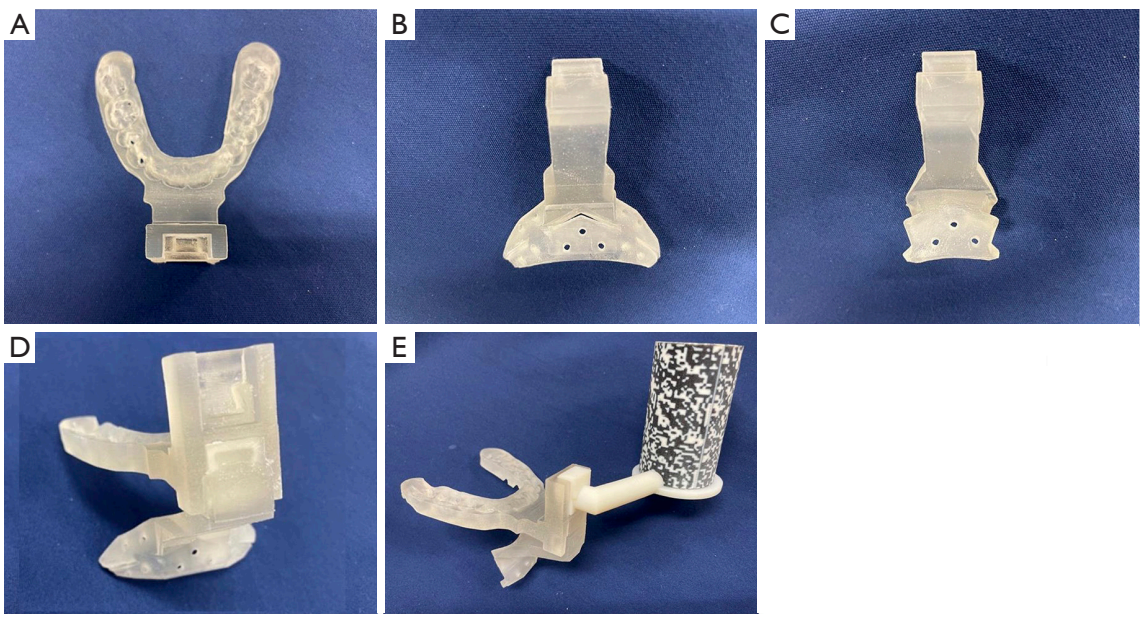

Figure 4 Three-dimensional devices made by computer-aided manufacturing with a 3D printable biocompatible resin: (A) surgical splint; (B) osteotomy device; (C) repositioning device; (D) surgical splint connected to the osteotomy device; (E) surgical splint connected to the repositioning device; the osteotomy device and repositioning device were customized in each case. 3D, three-dimensional.

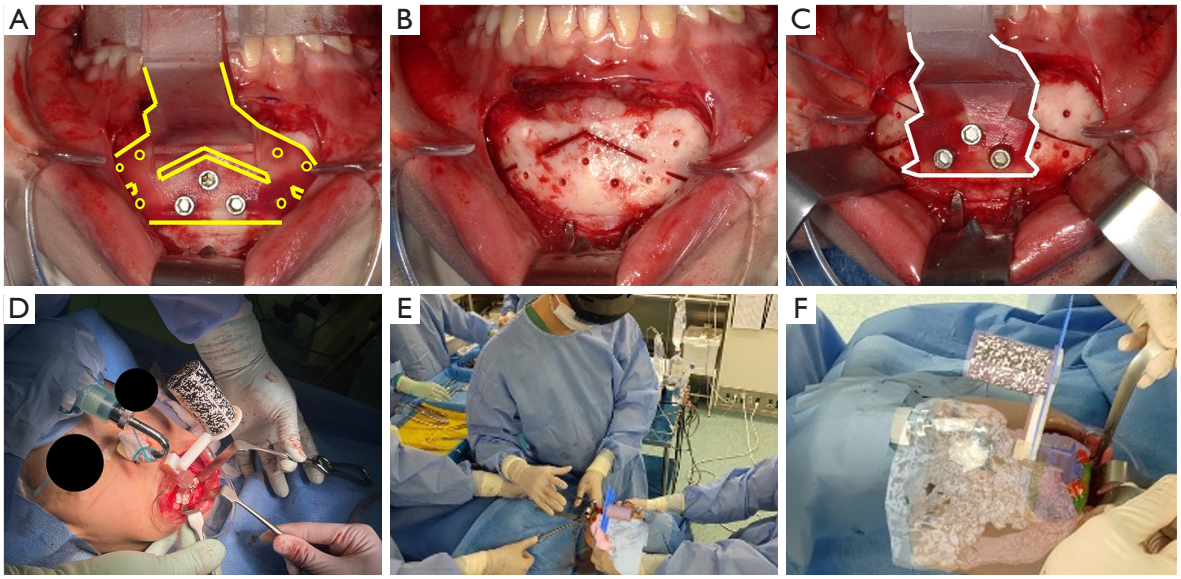

Figure 5 Intraoperative view: (A) intraoperative view of the osteotomy device (yellow) *in situ*. This is used to predrill the drill holes and perform the virtually planned osteotomy; (B) intraoperative view after marking the osteotomy lines; (C) intraoperative view of the repositioning device (white) *in situ*; (D) intraoperative view of the repositioning device with the marker; (E) operators wearing HoloLens2 headsets can share the hologram and manipulate it using gestures and voice commands; (F) the operating field and the application can be aligned automatically by fabricating the markers, and the HoloLens2 device recognizes the markers.

specialists of the Japanese Society of Oral and Maxillofacial Surgeons (JSOMS) at the time the study began and had more than 15 years of experience. They were also involved in at least 50 to 100 orthognathic surgeries per year during this period. The directions of movement of the chin fragments are presented in *Table 1*. An intraoral gingivobuccal incision was made between the distal bilateral canine teeth for all genioplasty procedures. After exposing the bony surface, splints were placed on the upper and lower teeth, and an osteotomy device was placed at the junction site. Three screws were inserted and temporarily fixed to the central screw hole (*Figure 5A,5B*). After osteotomy, the guide hole for the fixation screw was drilled, the osteotomy device was removed, and mobilization of the chin segment was confirmed. Next, the osteotomy device was replaced with a repositioning device (*Figure 5C*), the chin segment was repositioned to insert the screws into the repositioning screw holes, and the chin fragment was temporarily fixed using two metal plates. The registration marker was connected to the splint junction site (*Figure 5D*), and the bone fragment positions were confirmed to match the preoperative planning hologram using the HoloLens 2 (*Figure 5E,5F*). Finally, the main fixation was performed with two absorbable four-hole plates (SuperFixsorb® MX, Teijin Medical Technology, Osaka, Japan), and the repositioning device was removed.

Preoperative procedure—Microsoft® HoloLens 2

We created an MR hologram application for an HMD (HoloLens 2; Microsoft, Washington, USA) using open-source Blender 3D software (Blender Foundation, Amsterdam, Netherlands) and Holoeyes MD (Holoeyes, Tokyo, Japan) based on the STL data of the VSP. The application was installed on Microsoft® HoloLens 2, and the hologram was projected through Microsoft® HoloLens 2 onto the surgical field. Holograms were superimposed. Normally, a hologram projection onto a living body is registered manually using HMDs; however, in our previous studies, we established a method of superimposition with registration markers (21,22). During surgery, the surgeon wears the HoloLens 2 and checks the MR application and the surgical field. The surgeon had the ability to change the size, angle, and transparency of the hologram, switch freely between segments to be displayed, and view any cross-section with a finger gesture. This allowed the surgeon to confirm during surgery that the bone fragment had been repositioned as planned, and the surgeons corrected

and removed the error when it was identified using superimposed MR.

Evaluation

CT was performed 1 month after genioplasty to evaluate surgical outcomes (6,23). The accuracy of bone fragment repositioning was evaluated by comparing the chin bone fragment of the 3D-CT model of the actual postoperative outcome (T1) to that of the 3D-CT model of the VSP (Tv). Postoperative CT data were imported into the segmentation software Mimics (Materialize, Leuven, Belgium) to create T1, which was superimposed on Tv using GOM Inspect (GOM, Braunschweig, Germany) for comparison. Mandibular superimposition was performed in the area not moved by genioplasty, that is, the distal mandibular region, which includes the mandibular condyle above the surgical region (24,25). The region of interest was a bone fragment of the chin. The evaluation was performed using the "reversed" routine developed by Xia *et al.* (24) and Hsu *et al.* (25). Few anatomical structures exist in the mental region; therefore, three independent landmarks (pogonion and bilateral buccal corner point "Rt/Lt"; the intersection of the left and right first premolar root apex extensions and the mandibular submargin) at Tv and T1 were digitized and set to coordinates to define the position and orientation of the fragment in 3D space. The landmark-digitized Tv was superimposed onto the corresponding segment of T1 using the best-fit method, and a comparative evaluation was performed by measuring the differences in the distance and tilt of the corresponding landmarks. First, three arbitrary landmarks (pogonion Pog and wing points Rt and Lt on the left and right sides of the bone fragment) were set and digitized on the fragment Tv of the chin designed in the preoperative VSP. Second, the Tv and the three Tv landmarks were duplicated and moved together to register on the surface of the mental area of the postoperative CT using the surface best-fit method and were digitized as T1 and the three T1 landmarks. Finally, T1 was moved back to the VSP along with the T1 landmarks. The coordinates of all landmarks were recorded. The centroid was calculated from each Tv and T1 landmark, and a coordinate axis was assigned to each landmark, with the centroid as the origin.

The three axes were set in the x-direction (mediolateral), y-direction (anteroposterior), and z-direction (superoinferior) (24-28) (*Figure 6*). In addition to the 3D surface analysis comparing the 3D models of Tv and T1, a point-based analysis was conducted to assess positional (mediolateral, anteroposterior, and superoinferior) and orientational (pitch, roll, and yaw) differences in the centroid by comparing the coordinate axes. The relationship between the main direction of movement of the chin bone fragment and the accuracy was investigated.

All calculations were performed automatically using GOM Inspect. The same operator performed measurements twice, and the average value was used as the evaluation value. The intraclass correlation coefficient was determined for the two sets of Tv measurements and for the two sets of T1 measurements in the 3D surface analysis and point-based analysis and the analysis was blinded; the correlation coefficient in each case was greater than 0.96. The analysis in this study was conducted using STL data, which inherently contains limitations in resolution and precision. While GOM Inspect allows for high-accuracy deviation analysis at the ±0.001 mm level, the actual precision of the analysis is influenced by factors such as hardware, the resolution of the STL data, and the scanning process. As a result, deviations below 0.05 mm, such as 0.03 mm reported in this study, fall within the precision limit of the STL data and should be interpreted with caution.

Statistical analysis

All statistical analyses were performed using IBM SPSS Statistics (version 23.0; IBM Corp., Armonk, NY, USA). The root mean square deviation (RMSD) and Bland-Altman method for the position and orientation of the postoperative position to the planned position were calculated as point-based analyses. In addition to descriptive statistics, the Mann-Whitney *U* test was used to assess the significance of differences in all directions between the experimental and control groups, and statistical significance was set at $P<0.05$. We considered positional differences of <1 mm and orientational differences of <4° as clinically inconsequential (29-31).

Results

Twenty-six patients with a mean age of 32.0 years were included. None of the patients had postoperative wound infection, root damage, or inferior alveolar nerve damage, and 0.008 g (1.65 g) was perceptible on the Semmes-Weinstein test performed 3 months postoperatively in cases of temporary sensory disturbance. Repositioning was performed in two groups: using only CAD/CAM technology in the control group (n=10), and using CAD/

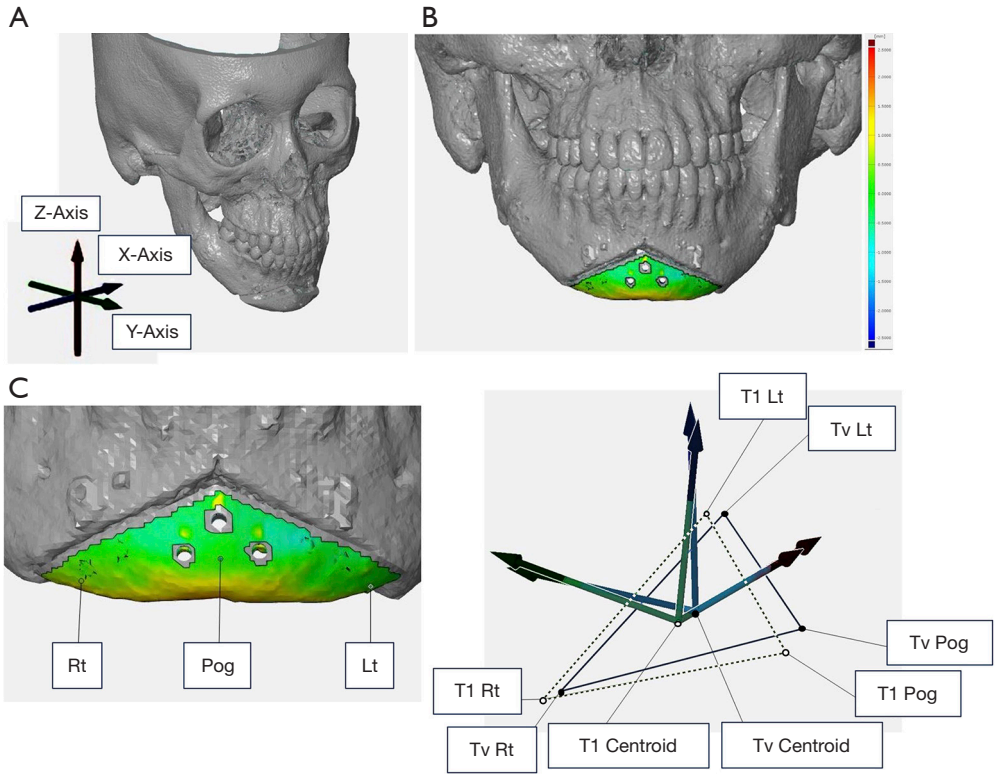

Figure 6 Reference plane and postoperative evaluations: (A) the reference plane was established, where the 3D-CT center was set as the middle point between the positions on both sides, the X-axis was set as the left-hand direction from the center, the Y-axis was set as the middle point that passes between the orbitales on both sides, and the Z-axis was set as the vertical cranial direction from the Frankfort horizontal plane; (B) a 3D surface analysis and a point-based analysis were used as the methods of evaluation; (C) the 3 points evaluated were as follows: pogonion (Pog), right lateral point of the chin segment (Rt), left lateral point of the chin segment (Lt). 3D, three-dimensional; CT, computed tomography; T1, the postoperative outcome; Tv, the actual postoperative outcome; POM1, postoperative month 1.

CAM with additional MR technology in the experimental group (n=16). Four types of CAD/CAM devices were designed based on VSP: a surgical splint with a connector, an osteotomy device, a repositioning device, and a novel registration marker. We used surgical devices designed and manufactured using VSP, while MR holograms created from the VSP data on Holoeyes MD were projected onto the surgical field using HoloLens 2 to improve surgery accuracy. Postoperative evaluation was performed by comparing the Tv model with the T1 model at 1 month postoperatively using 3D surface analysis, RMSD, and the Bland-Altman method to report translation and orientation differences in bone fragment repositioning in genioplasty. Registration for participation in this study did not result in any delays in surgery. The surgeons began surgery with the surgical device in place in all cases, and the operations proceeded smoothly.

3D surface analysis

The 3D surface analysis revealed that the percentage of data points with errors within 2 mm ranged from 62.20% to 100.00% in the control group and from 99.30% to 100.00% in the experimental group. The mean percentage of data points with errors within 2 mm was 92.12% for the control group and 99.81% for the experimental group. For errors within 1 mm, the percentage of data points ranged from 28.50% to 98.90% in the control group and from 55.10% to 99.60% in the experimental group, with mean percentages of 67.36% and 85.60%, respectively (*Table 2*). The results showed a statistically significant difference in errors within 1 mm between groups (P=0.047) (*Figure 7*). The combination of CAD/CAM and MR enabled accurate genioplasty. A slight decrease in accuracy was observed in cases involving advancement, setback, and rotation.

Point-based analysis

In the experimental group, the largest positional deviation between Tv and T1 was observed in the anteroposterior direction: the RMSD was 1.20 mm, with a mean ± standard deviation of −0.81±0.91 mm, a lower limit of −1.30 mm, and an upper limit of −0.32 mm (*Table 3*). The largest orientation deviation was in the pitch direction: the RMSD was 6.78°, with a mean ± standard deviation of 4.40°±5.16°, a lower limit of 1.56°, and an upper limit of 7.24°.

In the control group, the largest positional deviation was also in the anteroposterior direction: the RMSD was 1.78 mm, with a mean ± standard deviation of −0.97±1.58 mm, a lower limit of −2.10 mm, and an upper limit of 0.16 mm. The largest orientation deviation was in the pitch direction: the RMSD was 6.04°, with a mean ± standard deviation of 3.73°±4.75°, a lower limit of 0.14°, and an upper limit of 7.31° (*Table 4*).

Both groups tended to exhibit less accuracy in the anteroposterior and pitch directions. A statistically significant difference in yaw was observed between the groups (P=0.003) (*Figure 8*), although the difference in accuracy overall was not statistically significant. Since this time we are using a repositioning device and absorbable plate made from biocompatible resin, it is easy for the surrounding soft tissue, such as the muscles, to be affected during surgery, but it is difficult to reflect these effects in VSP. If there is a statistically significant difference, it is useful in that it is possible to confirm whether the bone fragment has been brought to the position actually assumed before surgery by using MR, and it is possible to improve the reproducibility of VSP. Some reported deviations, such as 0.03 mm, fall within the precision limit of the STL data used in this study. While GOM Inspect achieves high-accuracy deviation analysis (±0.001 mm), the actual precision of the results is influenced by factors such as hardware, the resolution of the STL data, and the scanning process. Therefore, deviations below the precision level of the STL data (e.g., 0.05 mm) should be interpreted with caution.

Table 2 3D surface analysis between Tv and T1

3D surface	Number of groups	Error <2 mm	Error <1 mm
CAD/CAM	10	92.12%	67.36%
CAD/CAM + MR	16	99.81%	85.60%

3D, three-dimensional; CAD/CAM, computer-aided design/computer-aided manufacturing; MR, mixed reality; T1, the postoperative outcome; Tv, the actual postoperative outcome.

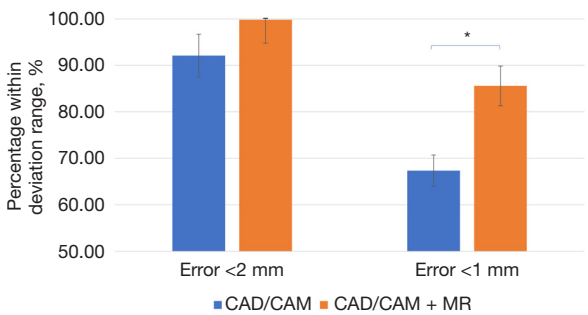

Figure 7 3D surface analysis between Tv and T1 (P<0.05). *, P value <0.5. 3D, three-dimensional; CAD/CAM, computer-aided design/computer-aided manufacturing; MR, mixed reality; T1, the postoperative outcome; Tv, the actual postoperative outcome.

Table 3 Positional differences between Tv and T1 (mm)

Group	Position	RMSD	Mean	SD	95% limits of agreement		Min	Max
					Lower	Upper		
CAD/CAM	Mediolateral (X-axis)	0.89	−0.32	0.87	−0.94	0.30	−1.41	0.93
	Anteroposterior (Y-axis)	1.78	−0.97	1.58	−2.10	0.16	−4.63	0.83
	Superoinferior (Z-axis)	1.03	0.24	1.05	−0.51	0.99	−2.19	1.41
CAD/CAM + MR	Mediolateral (X-axis)	0.69	−0.17	0.69	−0.53	0.20	−1.46	1.47
	Anteroposterior (Y-axis)	1.20	−0.81	0.91	−1.30	−0.32	−2.11	0.70
	Superoinferior (Z-axis)	0.77	0.19	0.77	−0.22	0.60	−1.07	2.06

CAD/CAM, computer-aided design/computer-aided manufacturing; MR, mixed reality; RMSD, root mean square deviation; SD, standard deviation; T1, the postoperative outcome; Tv, the actual postoperative outcome.

Table 4 Orientational differences between Tv and T1 (degrees)

Group	Orientation	RMSD	Mean	SD	95% limits of agreement		Min	Max
					Lower	Upper		
CAD/CAM	Pitch	6.04	3.73	4.75	0.14	7.31	−1.93	11.42
	Roll	1.97	0.24	1.95	−1.23	1.71	−3.4	3.03
	Yaw	3.30	1.64	2.86	−0.52	3.79	−3.68	5.81
CAD/CAM + MR	Pitch	6.78	4.40	5.16	1.56	7.24	−7.42	13.86
	Roll	2.43	1.21	2.11	0.05	2.37	−3.78	4.38
	Yaw	1.93	−1.27	1.45	−2.07	−0.47	−4.38	1.48

CAD/CAM, computer-aided design/computer-aided manufacturing; MR, mixed reality; RMSD, root mean square deviation; SD, standard deviation; T1, the postoperative outcome; Tv, the actual postoperative outcome.

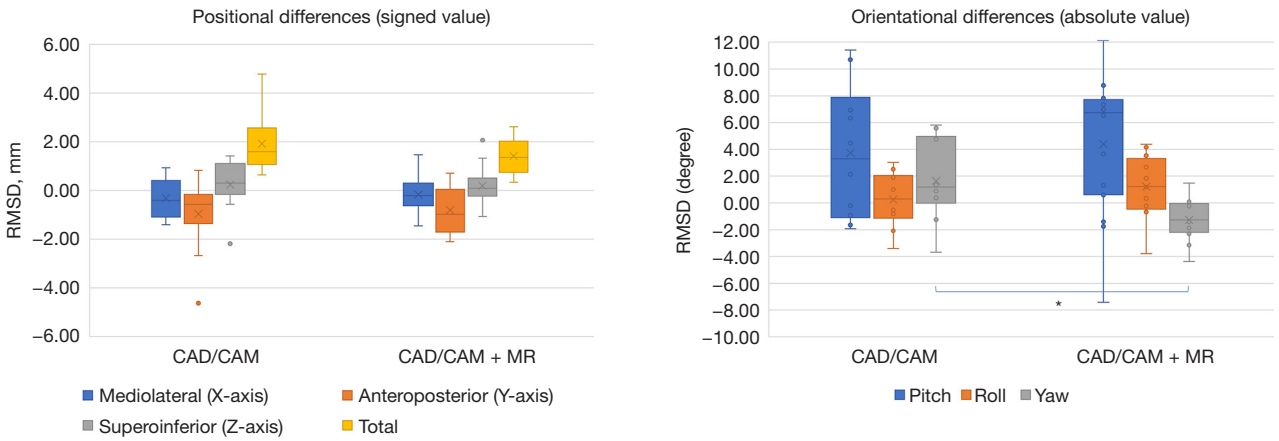

Figure 8 Signed value difference between Tv and T1 (P<0.05). The accuracy at each point was calculated regarding the XYZ axes. Positive values represent overcorrection and negative values represent undercorrection of the planned position of the fragment. *, P value <0.5. CAD/CAM, computer-aided design/computer-aided manufacturing; MR, mixed reality; RMSD, root mean square deviation; T1, the postoperative outcome; Tv, the actual postoperative outcome.

Table 5 Types and numbers of main directions of movement of chin fragments

Group	Setback	Advancement	Rotation	Upward	Setback + advancement
Total	3	12	7	4	15
CAD/CAM	2	5	2	1	7
CAD/CAM + MR	1	7	5	3	8

CAD/CAM, computer-aided design/computer-aided manufacturing; MR, mixed reality.

By the main direction of the movement of the fragment

The types and numbers of the main movement directions of the fragments are listed in *Table 5*. The error by direction of movement of the bone fragments is shown in *Tables 6*,7, in which errors over 1 mm or 4° and under −1 mm or −4° are shaded.

Discussion

Genioplasty is an important type of orthognathic surgery that affects the shape of the facial soft tissue. Genioplasty involves a subjective evaluation of the cosmetic appearance and has a significant bearing on functional aspects such as lip closure (32-34). Therefore, patients are interested in

Table 6 Positional differences between Tv and T1 (degrees) by main directions

Group	Position	Setback			Advancement			Rotation			Upward			Setback + advancement		
		RMSD	Mean	SD	RMSD	Mean	SD	RMSD	Mean	SD	RMSD	Mean	SD	RMSD	Mean	SD
Total	Mediolateral (X-axis)	0.85	−0.28	0.80	0.81	−0.18	0.79	0.84	−0.27	0.79	0.28	−0.24	0.14	0.82	−0.20	0.80
	Anteroposterio (Y-axis)	0.60	−0.43	0.42	1.94†	−1.49†	1.25	0.92	−0.42	0.81	0.78	−0.12	0.77	1.76†	−1.28†	1.21
	Superoinferior (Z-axis)	1.45†	1.23†	0.77	0.65	0.20	0.61	1.08†	−0.17	1.07	0.37	0.13	0.35	0.87	0.41	0.77
CAD/CAM	Mediolateral (X-axis)	1.01†	−0.59	0.83	0.95	−0.07	0.95	0.80	−0.8	0.04	0.06	−0.06	0.00	0.97	−0.22	0.94
	Anteroposterio (Y-axis)	0.73	−0.70	0.23	2.42†	−1.74†	1.68	0.79	0.04	0.79	0.36	0.35	0.00	2.08†	−1.44†	1.50
	Superoinferior (Z-axis)	1.01†	0.81	0.6	0.82	0.42	0.70	1.56†	−0.93	1.26	0.35	0.53	0.00	0.88	0.53	0.70
CAD/CAM + MR	Mediolateral (X-axis)	0.34	0.34	0.00	0.70	−0.26	0.65	0.85	−0.06	0.85	0.32	−0.3	0.12	0.67	−0.18	0.64
	Anteroposterio (Y-axis)	0.09	0.09	0.00	1.51†	−1.31†	0.76	0.96	−0.61	0.75	0.88	−0.28	0.83	1.42†	−1.13†	0.85
	Superoinferior (Z-axis)	2.06†	2.06†	0.00	0.49	0.05	0.49	0.81	0.14	0.80	0.30	−0.01	0.30	0.86	0.30	0.81

Values below 0.05 mm fall within the precision limit of the STL data and should be interpreted with caution. †, error >1 mm. CAD/CAM, computer-aided design/computer-aided manufacturing; MR, mixed reality; RMSD, root mean square deviation; SD, standard deviation; STL, Standard Tessellation Language; T1, the postoperative outcome; Tv, the actual postoperative outcome.

Table 7 In orientational differences between Tv and T1 (degrees) by main directions

Group	Position	Setback			Advancement			Rotation			Upward			Setback + advancement		
		RMSD	Mean	SD	RMSD	Mean	SD	RMSD	Mean	SD	RMSD	Mean	SD	RMSD	Mean	SD
Total	Pitch	5.43†	4.64†	5.29	7.65†	5.53†	2.82	5.69†	3.05	4.80	4.55†	1.51	4.30	7.26†	5.35†	4.91
	Roll	1.66	−0.24	1.72	2.05	1.12	1.64	2.99	0.44	2.96	1.72	1.51	0.83	1.97	0.84	1.57
	Yaw	2.92	−1.12	2.75	2.59	1.27	0.67	2.61	−1.70	1.87	1.90	−0.99	1.05	2.66	0.79	2.48
CAD/CAM	Pitch	6.64†	6.63†	0.30	7.05†	3.87	5.89†	3.50	3.30	1.17	1.93	−1.93	0.00	6.94†	4.66†	4.29
	Roll	1.99	−0.09	1.99	1.82	0.75	1.66	2.55	−1.10	2.3	1.01	1.01	0.00	1.87	0.51	1.57
	Yaw	3.43	2.82	1.94	3.76	2.60	2.71	2.62	−1.65	2.03	1.01	1.01	0.00	3.66	2.67	2.07
CAD/CAM + MR	Pitch	0.67	0.67	0.00	8.06†	6.72†	4.45†	6.36†	2.94	5.63†	5.14†	2.65	4.40†	7.54†	5.96†	3.99
	Roll	0.54	−0.54	0.00	2.19	1.37	1.71	3.15	1.06	2.97	1.90	1.68	0.90	2.06	1.13	1.55
	Yaw	1.48	1.48	0.00	1.20	−0.91	0.90	2.60	−2.04	1.53	2.12	−1.75	1.19	1.24	−0.61	0.79

†, error >4 degrees. CAD/CAM, computer-aided design/computer-aided manufacturing; MR, mixed reality; RMSD, root mean square deviation; SD, standard deviation; T1, the postoperative outcome; Tv, the actual postoperative outcome.

this type of surgery. This surgery requires preoperative simulation to obtain patient consensus and accuracy.

In recent years, various digital technologies have been widely applied to surgery in the maxillofacial region (8-13), and their surgical accuracy and effectiveness have been widely reported. Various approaches have been reported in the field of orthognathic surgery, including the use of one or both osteotomy and repositioning devices (22,25,35-39), navigation systems (40), and patient-specific implants (PSIs) using 3D metal printing (41-43). These approaches have demonstrated significant improvements over conventional surgical techniques and have been reported to safely protect important anatomical structures, such as the mental nerve and tooth root, and to avoid postoperative numbness and dental complications (7). However, few reports address the accuracy of these methods, and limited studies include a control group, considering that PSIs fabricated by 3D metal printing have long fabrication times and are costly (44-48). In addition, PSIs produced by 3D metal printing have not yet been clinically approved in Japan, and 3D

printers using biocompatible materials are the mainstream for surgical devices, as reported in the present study. Image-guided surgery (IGS) using a navigation system requires large and expensive equipment and repeated intraoperative calibrations. However, MR-equipped HMDs are relatively affordable and portable; therefore, they are currently employed for navigation in a variety of surgical procedures, and their accuracy has been reported (15,16,49). We previously established an automatic intraoperative registration method using this marker (22) and created a novel registration marker that was more compact than the former and did not obstruct the operative field for genioplasty (21).

Based on the study by Koyachi *et al.* (21,22), this study used 3D surface analysis and the Bland-Altman method to determine the accuracy of genioplasty using CAD/CAM in combination with MR technology (50). Traditionally, positional differences of <2 mm and orientational differences of <4° were considered clinically insignificant in the interpretation of accuracy in orthognathic surgery. However, the interpretation of accuracy measurement results has been based on positional differences of <1 mm in recent years (29-31).

In this study, the 3D surface analysis errors within 2 mm ranged from 62.22% to 100.00% (CAD/CAM group) and 99.30% to 100.00% (CAD/CAM + MR group), with mean errors of 92.12% *vs.* 99.81%, respectively. Errors within 1 mm ranged between 28.50–98.9% (CAD/CAM group) *vs.* 55.1–99.6% (CAD/CAM + MR group), with mean errors of 67.36% *vs.* 85.60%, respectively. A statistically significant difference in the errors within 1 mm was observed between the groups (P=0.047). A slight decrease in accuracy was observed in the cases of complex movement, advancement, and setback of the bone fragments. The mean error within 1 mm for simple objects increased to 89.97% (74.80–99.60%) in the experimental group. Currently, few reports evaluate genioplasty using 3D surface analysis, and previous studies on Le Fort I osteotomies performed using VSP devices or 3D-printed metal PSIs have reported alignment errors of <2 mm on the bone surface, ranging between 62–100%, with a mean of 83.8–92.7% (40,51). Koyachi *et al.* reported errors within 2 mm in their maxillary repositioning method, with a mean of 90.3% (22). Our study provides more accurate results than previous reports. In the 3D surface analysis, CAD/CAM devices improved the accuracy of the surgery, and the addition of MR improved the accuracy more significantly than CAD/CAM alone.

Point-based analysis using the RMSD and Bland-Altman methods showed that the difference in position was <1 mm in all axes in both groups for the signed mean by comparing Tv and T1. The RMSD improved in all axes in the experimental group and was <1 mm in the anteroposterior and superoinferior directions. Thus, the CAD/CAM device improved the surgical accuracy in all three axes, and the addition of MR improved the accuracy over CAD/CAM alone in all three axes. Both groups had roll and yaw errors within 4°; however, the addition of MR significantly improved the yaw accuracy. This suggests that MR improves the clinical accuracy. When evaluated by the main movement direction, differences in the anteroposterior direction and pitch were significant in cases involving anteroposterior movement of the bone fragments of the chin. Particularly in cases involving anterior movement of the bone fragments, the RMSD was improved, but the accuracy in the anteroposterior direction was negative in both groups, and the bone fragments were positioned more posteriorly than planned. This suggests that the anteroposterior movement of bone fragments in genioplasty may require more movement than planned, as it significantly impacts orientation differences more than rotation or upward movement. In the intraoperative 3D confirmation using MR, errors in the mediolateral, superoinferior, roll, and yaw directions were easily detected, especially in the yaw direction, even when the VSP data were superimposed.

In the previous cases using PSI and metal plates, the largest difference in position was in the anteroposterior direction, with an RMSD of 0.69–1.11 mm, a signed mean of –0.84 to 0.27 mm, an upper limit of 2.94 mm, and a lower limit of –2.28 mm, and the largest difference in orientation was in the pitch direction, with an RMSD of 2.63°, with a signed mean of –1.51° to 1.76°, an upper limit of 3.81 mm, and a lower limit of –4.16° (6,43,52). Although no studies have evaluated the IGS accuracy in genioplasty, existing research on IGS accuracy in maxillary osteotomy reported RMSDs of 1.16 to 2.1 mm (53,54). Thus, the accuracy of this study is comparable to that of past PSI and IGS in terms of position error, with the difference in orientation occurring in the direction of pitch rotation.

This study has two limitations. The first limitation is the anatomy of the chin. Because the cortical bone of the chin is thicker than that of the maxilla, the osteotomy line of the buccal cortical bone is easily set when using an osteotomy device. However, determining the osteotomy position and direction of the lingual cortical bone is difficult and affects the control and repositioning of the bone fragment and bone interference. Furthermore, because the geniohyoid muscle

runs on the lingual side of the chin bone fragment, a fixation force is required for movements involving advancement, setback, and complex movements that resist the trajectory of the geniohyoid muscle (55). Therefore, in addition to CAD/CAM devices, MR may be useful for confirming the accuracy of the final position. The second limitation was the use of absorbable plates. Unlike the custom metal plates used in previous studies, absorbable plates are subject to gradual extension and material constraints, as reported by Ueki *et al.* (56). Therefore, the use of metal plates may need to be considered when performing genioplasty for long-term prognosis or genioplasty involving large amounts of bone fragment displacement. However, because the use of metal plates involves surgical removal and the associated risks, this technique, which involves absorbable plates and provides a high degree of accuracy, may be useful.

In addition to the high accuracy of the CAD/CAM device from a 3D printer alone, this method combined with MR technology enables intraoperative 3D evaluation and significantly improves the reproducibility of the position of hard tissue fragments. This is the first report on the accuracy and usefulness of MR for genioplasty and suggests that this method can be used to perform genioplasty with a high degree of accuracy. In the future, improving surgical accuracy will be essential, along with establishing a genioplasty technique that improves surgical safety. This can be achieved by increasing the information projected by MR, such as visualizing surrounding blood vessels, in combination with contrast-enhanced CT.

Conclusions

The use of MR in genioplasty enabled confirmation of spatial repositioning of the chin fragments and more accurate placement of the planned plate. This method improves the accuracy of fragment repositioning. Therefore, the combination of CAD/CAM and MR technology allows for intraoperative spatial verification of fragment movement according to preoperative VSP. This method has improved the technique's accuracy and VSP reproducibility, significantly contributing to surgical precision.

Acknowledgments

We would like to thank Meishin Electric Co., Inc. for the appropriate design of the devices and Holoeyes, Inc. for technical support during the creation of the MR application.

Footnote

Reporting Checklist: The authors have completed the CONSORT reporting checklist. Available at https://qims.amegroups.com/article/view/10.21037/qims-24-2333/rc

Trial Protocol: Available at https://qims.amegroups.com/article/view/10.21037/qims-24-2333/tp

Funding: This research was funded by JSPS KAKENHI (grant No. JP21K17123 to M.K.).

Conflicts of Interest: All authors have completed the ICMJE uniform disclosure form (available at https://qims.amegroups.com/article/view/10.21037/qims-24-2333/coif). M.K. reports that this work was supported by JSPS KAKENHI (grant No. JP21K17123). The other authors have no conflicts of interest to declare.

Ethical Statement: The authors are accountable for all aspects of the work in ensuring that questions related to the accuracy or integrity of any part of the work are appropriately investigated and resolved. This study was conducted in accordance with the Declaration of Helsinki (as revised in 2013). The study was approved by the Ethics Committee of Tokyo Dental College (No. 794, 844) and informed consent was obtained from all individual participants.

References

1. Da Silva HF, Marinho LF, Souza GA, Sverzut AT, Olate S, Asprino L, de Moraes M. About chin (genioplasty) surgery. Int J Morphol 2020;38:1120-7.
2. Nishioka GJ, Mason M, Van Sickels JE. Neurosensory disturbance associated with the anterior mandibular horizontal osteotomy. J Oral Maxillofac Surg 1988;46:107-10.
3. Khan M, Sattar N, Erkin M. Postoperative Complications

in Genioplasty and Their Association with Age, Gender, and Type of Genioplasty. Int J Dent 2021;2021:8134680.
4. Lindquist CC, Obeid G. Complications of genioplasty done alone or in combination with sagittal split-ramus osteotomy. Oral Surg Oral Med Oral Pathol 1988;66:13-6.
5. Lin L, Xu C, Shi Y, Zhou C, Zhu M, Chai G, Xie L. Preliminary clinical experience of robot-assisted surgery in treatment with genioplasty. Sci Rep 2021;11:6365.
6. Li B, Wei H, Zeng F, Li J, Xia JJ, Wang X. Application of A Novel Three-dimensional Printing Genioplasty Template System and Its Clinical Validation: A Control Study. Sci Rep 2017;7:5431.
7. Oth O, Durieux V, Orellana MF, Glineur R. Genioplasty with surgical guide using 3D-printing technology: A systematic review. J Clin Exp Dent 2020;12:e85-92.
8. Katsumi Y, Sugahara K, Matsunaga S, Odaka K, Mitomo K, Abe S, Koyachi M, Ito K, Takano M, Katakura A. Planning for orthognathic surgery at medical fabrication laboratory in Tokyo Dental College (Fab Lab TDC) Clinical Application of Full-Scale-Model made by 3-Dimensional Ink Jet Printer for Orthognathic Surgery. Oral Science in Japan 2016;2016:9-11.
9. Cui MX, Xiao LC, Yue J, Xue LF, Xiao WL. Effect of a digital guide on the positional accuracy of intermaxillary fixation screw implantation in orthognathic surgery. J Plast Reconstr Aesthet Surg 2022;75:e15-22.
10. Yuan P, Mai H, Li J, Ho DC, Lai Y, Liu S, Kim D, Xiong Z, Alfi DM, Teichgraeber JF, Gateno J, Xia JJ. Design, development and clinical validation of computer-aided surgical simulation system for streamlined orthognathic surgical planning. Int J Comput Assist Radiol Surg 2017;12:2129-43.
11. Kumari T, Ramanathan A. Digital technology in craniofacial surgery – historical perspectives to current applications. Dentistry Review 2022;2:100039.
12. Yang R, Li C, Tu P, Ahmed A, Ji T, Chen X. Development and Application of Digital Maxillofacial Surgery System Based on Mixed Reality Technology. Front Surg 2021;8:719985.
13. Sun R, Zhou Y, Malouta MZ, Cai Y, Shui C, Zhu L, Wang X, Zhu J, Li C. Digital surgery group versus traditional experience group in head and neck reconstruction: a retrospective controlled study to analyze clinical value and time-economic-social effect. World J Surg Oncol 2022;20:220.
14. Xu H, Zhang C, Shim YH, Li H, Cao D. Combined use of rapid-prototyping model and surgical guide in correction of mandibular asymmetry malformation patients with normal occlusal relationship. J Craniofac Surg 2015;26:418-21.
15. Chiacchiaretta P, Perrucci MG, Caulo M, Navarra R, Baldiraghi G, Rolandi D, Luzzi S, Del Maestro M, Galzio R, Ferretti A. A Dedicated Tool for Presurgical Mapping of Brain Tumors and Mixed-Reality Navigation During Neurosurgery. J Digit Imaging 2022;35:704-13.
16. Sugahara K, Koyachi M, Koyama Y, Sugimoto M, Matsunaga S, Odaka K, Abe S, Katakura A. Mixed reality and three dimensional printed models for resection of maxillary tumor: a case report. Quant Imaging Med Surg 2021;11:2187-94.
17. Koyama Y, Sugahara K, Koyachi M, Tachizawa K, Iwasaki A, Wakita I, Nishiyama A, Matsunaga S, Katakura A. Mixed reality for extraction of maxillary mesiodens. Maxillofac Plast Reconstr Surg 2023;45:1.
18. Sugahara K, Koyachi M, Tachizawa K, Iwasaki A, Matsunaga S, Odaka K, Sugimoto M, Abe S, Nishii Y, Katakura A. Using mixed reality and CAD/CAM technology for treatment of maxillary non-union after Le Fort I osteotomy: a case description. Quant Imaging Med Surg 2023;13:1190-9.
19. Sasaki T, Dehari H, Ogi K, Miyazaki A. Application of a mixed reality device to oral surgery. Advances in Oral and Maxillofacial Surgery 2022;8:100331.
20. Brunzini A, Mazzoli A, Pagnoni M, Mandolini M. An innovative mixed reality approach for maxillofacial osteotomies and repositioning. Virtual Reality 2023;27:3221-37.
21. Koyachi M, Sugahara K, Tachizawa K, Nishiyama A, Odaka K, Matsunaga S, Sugimoto M, Tachiki C, Nishii Y, Katakura A. Enhanced Precision in Genioplasty: A Novel Intraoperative Spatial Repositioning Using Computer-Aided Design and Manufacturing Technology and a Holographic Mixed Reality Application. J Clin Med 2023;12:7408.
22. Koyachi M, Sugahara K, Odaka K, Matsunaga S, Abe S, Sugimoto M, Katakura A. Accuracy of Le Fort I osteotomy with combined computer-aided design/computer-aided manufacturing technology and mixed reality. Int J Oral Maxillofac Surg 2021;50:782-90.
23. Swennen GR, Mollemans W, Schutyser F. Three-dimensional treatment planning of orthognathic surgery in the era of virtual imaging. J Oral Maxillofac Surg 2009;67:2080-92.
24. Xia JJ, Gateno J, Teichgraeber JF, Christensen AM, Lasky RE, Lemoine JJ, Liebschner MA. Accuracy of the computer-aided surgical simulation (CASS) system in the

treatment of patients with complex craniomaxillofacial deformity: A pilot study. J Oral Maxillofac Surg 2007;65:248-54.
25. Hsu SS, Gateno J, Bell RB, Hirsch DL, Markiewicz MR, Teichgraeber JF, Zhou X, Xia JJ. Accuracy of a computer-aided surgical simulation protocol for orthognathic surgery: a prospective multicenter study. J Oral Maxillofac Surg 2013;71:128-42.
26. Xia JJ, Gateno J, Teichgraeber JF. New clinical protocol to evaluate craniomaxillofacial deformity and plan surgical correction. J Oral Maxillofac Surg 2009;67:2093-106.
27. Xia JJ, Gateno J, Teichgraeber JF, Yuan P, Chen KC, Li J, Zhang X, Tang Z, Alfi DM. Algorithm for planning a double-jaw orthognathic surgery using a computer-aided surgical simulation (CASS) protocol. Part 1: planning sequence. Int J Oral Maxillofac Surg 2015;44:1431-40.
28. Xia JJ, Gateno J, Teichgraeber JF, Yuan P, Li J, Chen KC, Jajoo A, Nicol M, Alfi DM. Algorithm for planning a double-jaw orthognathic surgery using a computer-aided surgical simulation (CASS) protocol. Part 2: three-dimensional cephalometry. Int J Oral Maxillofac Surg 2015;44:1441-50.
29. Donatsky O, Bjørn-Jørgensen J, Holmqvist-Larsen M, Hillerup S. Computerized cephalometric evaluation of orthognathic surgical precision and stability in relation to maxillary superior repositioning combined with mandibular advancement or setback. J Oral Maxillofac Surg 1997;55:1071-9; discussion 1079-80.
30. Padwa BL, Kaiser MO, Kaban LB. Occlusal cant in the frontal plane as a reflection of facial asymmetry. J Oral Maxillofac Surg 1997;55:811-6; discussion 817.
31. Ong TK, Banks RJ, Hildreth AJ. Surgical accuracy in Le Fort I maxillary osteotomies. Br J Oral Maxillofac Surg 2001;39:96-102.
32. Precious DS, Delaire J. Correction of anterior mandibular vertical excess: the functional genioplasty. Oral Surg Oral Med Oral Pathol 1985;59:229-35.
33. Saponaro G, Gasparini G, Boniello R, Pelo S, Doneddu P, Todaro M, D'Amato G, Garagiola U, Grippaudo C, Moro A. The Rules of Attractiveness: A Study on the Lower Facial Third. J Craniofac Surg 2018;29:1945-6.
34. Lee EI. Aesthetic alteration of the chin. Semin Plast Surg 2013;27:155-60.
35. Wei X, Zheng J, Bu L, Luo Y, Qiu Y, Yang C. Digital template-guided genioplasty for patients with jaw deformity resulting from temporomandibular joint ankylosis: A comparison between single- and double-layer genioplasty. Int J Oral Maxillofac Surg 2023;52:1057-63.
36. Costa PJC, Demétrio MS, Nogueira PTBC, Rodrigues LR, Júnior PDR. A New Proposal for Three-Dimensional Positioning of the Chin Using a Single Computer-Aided Design/Computer-Aided Manufacturing Surgical Guide. J Craniofac Surg 2018;29:1963-4.
37. Di Brigida L, Naddeo A, Cappetti N, Borri A, Cortese A. Computer Aided Orthognathic Surgery: A General Method for Designing and Manufacturing Personalized Cutting/Repositioning Templates. Appl Sci 2022;12:3600.
38. Lim SH, Kim MK, Kang SH. Genioplasty using a simple CAD/CAM (computer-aided design and computer-aided manufacturing) surgical guide. Maxillofac Plast Reconstr Surg 2015;37:44.
39. Li B, Zhang L, Sun H, Yuan J, Shen SG, Wang X. A novel method of computer aided orthognathic surgery using individual CAD/CAM templates: a combination of osteotomy and repositioning guides. Br J Oral Maxillofac Surg 2013;51:e239-44.
40. Badiali G, Roncari A, Bianchi A, Taddei F, Marchetti C, Schileo E. Navigation in Orthognathic Surgery: 3D Accuracy. Facial Plast Surg 2015;31:463-73.
41. Greenberg S, Buchbinder D, Turner MD, Dhillon P, Afshar AA. Three-Dimensional Repositioning of the Maxilla in Orthognathic Surgery Using Patient-Specific Titanium Plates: A Case Series. J Oral Maxillofac Surg 2021;79:902-13.
42. Suojanen J, Leikola J, Stoor P. The use of patient-specific implants in orthognathic surgery: A series of 30 mandible sagittal split osteotomy patients. J Craniomaxillofac Surg 2017;45:990-4.
43. Li B, Wang S, Wei H, Zeng F, Wang X. The use of patient-specific implants in genioplasty and its clinical accuracy: a preliminary study. Int J Oral Maxillofac Surg 2020;49:461-5.
44. Figueiredo CE, Paranhos LR, da Silva RP, Herval ÁM, Blumenberg C, Zanetta-Barbosa D. Accuracy of orthognathic surgery with customized titanium plates-Systematic review. J Stomatol Oral Maxillofac Surg 2021;122:88-97.
45. Williams A, Walker K, Hughes D, Goodson AMC, Mustafa SF. Accuracy and cost effectiveness of a waferless osteotomy approach, using patient specific guides and plates in orthognathic surgery: a systematic review. Br J Oral Maxillofac Surg 2022;60:537-46.
46. Huang MF, Alfi D, Alfi J, Huang AT. The Use of Patient-Specific Implants in Oral and Maxillofacial Surgery. Oral Maxillofac Surg Clin North Am 2019;31:593-600.
47. Pascal E, Majoufre C, Bondaz M, Courtemanche A, Berger

M, Bouletreau P. Current status of surgical planning and transfer methods in orthognathic surgery. J Stomatol Oral Maxillofac Surg 2018;119:245-8.
48. Van den Bempt M, Liebregts J, Maal T, Bergé S, Xi T. Toward a higher accuracy in orthognathic surgery by using intraoperative computer navigation, 3D surgical guides, and/or customized osteosynthesis plates: A systematic review. J Craniomaxillofac Surg 2018;46:2108-19.
49. Matyash I, Kutzner R, Neumuth T, Rockstroh M. Accuracy measurement of HoloLens2 IMUs in medical environments. Curr Dir Biomed Eng 2021;7:633-6.
50. Bland JM, Altman DG. Statistical methods for assessing agreement between two methods of clinical measurement. Lancet 1986;1:307-10.
51. Mazzoni S, Bianchi A, Schiariti G, Badiali G, Marchetti C. Computer-aided design and computer-aided manufacturing cutting guides and customized titanium plates are useful in upper maxilla waferless repositioning. J Oral Maxillofac Surg 2015;73:701-7.
52. Rückschloß T, Ristow O, Kühle R, Weichel F, Roser C, Aurin K, Engel M, Hoffmann J, Freudlsperger C. Accuracy of laser-melted patient-specific implants in genioplasty - A three-dimensional retrospective study. J Craniomaxillofac Surg 2020;48:653-60.
53. Berger M, Nova I, Kallus S, Ristow O, Freudlsperger C, Eisenmann U, Dickhaus H, Engel M, Hoffmann J, Seeberger R. Can electromagnetic-navigated maxillary positioning replace occlusional splints in orthognathic surgery? A clinical pilot study. J Craniomaxillofac Surg 2017;45:1593-9.
54. Lee SJ, Woo SY, Huh KH, Lee SS, Heo MS, Choi SC, Han JJ, Yang HJ, Hwang SJ, Yi WJ. Virtual skeletal complex model- and landmark-guided orthognathic surgery system. J Craniomaxillofac Surg 2016;44:557-68.
55. Kim S, Jo JH, Sri L, Dharma MAT, Park YS. Geniohyoid muscle: anatomy and clinical implications in dentistry. Int J Morphol 2023;41:851-7.
56. Ueki K, Moroi A, Yoshizawa K. Stability of the chin after advancement genioplasty using absorbable plate and screws with template devices. J Craniomaxillofac Surg 2019;47:1498-503.

Cite this article as: Tachizawa K, Sugahara K, Koyachi M, Odaka K, Matsunaga S, Sugimoto M, Katakura A. Enhancing the accuracy of genioplasty using mixed reality and computer-aided design/manufacturing: a randomized controlled trial. Quant Imaging Med Surg 2025;15(5):4774-4790. doi: 10.21037/qims-24-2333